Electrically Large Dual-Loop Antenna for UHF Near-Field RFID Reader

Jin Shi, Xianming Qing, *Member, IEEE*, Zhi Ning Chen, *Fellow, IEEE*, and Chean Khan Goh

Abstract—An electrically large dual-loop antenna is proposed for ultra high frequency (UHF) near-field radio frequency identification (RFID) readers. The proposed antenna is composed of a main loop and a parasitic loop wherein the loops are constructed using segmented lines with distributed capacitors. The parasitic loop enhances and uniforms the magnetic field distribution in the central portion of the larger main loop so that the perimeter of interrogation zone of the dual-loop antenna can be extended up to three operating wavelengths. The measurement shows that a dual-loop antenna prototype printed onto a piece of FR4 printed circuit board (PCB) achieves good impedance matching over the frequency range of 845–928 MHz and produces strong and uniform magnetic field distribution with an interrogation zone of 250 mm × 250 mm. A parametric study is carried out to provide the guidelines for the antenna design.

Index Terms—Distributed capacitor, electrically large, loop antenna, parasitic loop, radio frequency identification (RFID), segmented loop, ultrahigh frequency (UHF).

I. INTRODUCTION

R ADIO FREQUENCY identification (RFID) is a wireless identification and tracking technology applied in warehouse, supply chain, control system, and automation process [1]–[3]. Currently, ultrahigh frequency (UHF) near-field RFID technology has received a lot of attention because of the promising opportunities in item-level RFID applications such as sensitive products tracking, pharmaceutical logistics, transport, medical products, and bio-sensing applications [4]–[8]. The design challenge of the UHF near-field RFID reader antennas is to provide the efficient tag detection with a large interrogation zone, i.e., generate a strong and uniform magnetic field distribution over a large area. The larger interrogation zone of the antenna offers the system higher speed, i.e., detect more tags with shorter time.

In most of the near-field RFID applications, the interaction between the RFID reader and tags is based on inductive coupling [9], [10]. The conventional solid-line loop antennas have been used as reader antennas in low frequency (LF)/high frequency (HF) RFID systems for years. Usually, these electrically-small loops (i.e., the perimeter of a loop antenna $C < \lambda/2\,\pi$, where λ is the operating wavelength in free space) can produce strong and uniform magnetic field in the region near to the antenna. However, such a solid-line loop antenna is unable to produce a uniform magnetic field over the near-field region of an electrically large antenna, where the perimeter of the interrogation zone is larger than one wavelength because the current features phase-inversion along the loop.

Some work has been reported to address the design of electrically large loop antennas for UHF near-field RFID applications. The key design challenge is to realize strong and uniform magnetic field distribution in the central portion of the antennas. Dobkin *et al.* presented a segmented loop antenna loaded with lumped capacitors in 2007 [11]. Oliver proposed three broken-loop antennas using different coupled lines in 2008 [12]–[14]. Using distributed capacitors [15], [16] or dash-line [17]–[19] to configure a segmented loop antenna or embedding phase shifter into solid-line loops [20], the current along the loop antennas can be kept in phase along the loop even though the perimeter of the loop is about two operating wavelengths at 900 MHz. Moreover, a dual-dipole antenna has been reported to compose a loop for providing in-phase current performance as well [21]. To date, the maximum interrogation zone of the reported UHF near-field RFID reader antennas has reached around 160×160 mm^2 [20].

In this paper, a dual-loop near-field antenna is proposed to further enlarge the interrogation zone up to 250 mm × 250 mm at UHF bands. The proposed antenna is investigated numerically and validated experimentally. A parametric study is carried out to explore the operating mechanism of the antenna and provide the guidelines for antenna design and optimization.

II. DUAL-LOOP ANTENNA

A. Antenna Configuration

The proposed dual-loop antenna printed on FR4 printed circuit board (PCB) (thickness of 0.5 mm, relative dielectric constant of 4.4, and loss tangent of 0.02) is shown in Fig. 1. A Cartesian coordinate system is oriented such that the upper surface of the FR4 PCB lies in the $x - y$ plane and the center of the outer loop is at the origin of the coordinate system. The internal area (250 mm × 250 mm) of the main loop is indicated as the interrogation zone with a perimeter of 1000 mm or about three wavelengths at 915 MHz. The antenna is fed by a parallel strip line printed on the opposite sides of the substrate. An impedance matching network comprising coplanar stripline stubs is adopted to match the antenna to the 50-Ω feed. The

J. Shi, X. Qing, and C. K. Goh are with the Institute for Infocomm Research, A*STAR, Singapore (e-mail: jshi@i2r.a-star.edu.sg; qingxm@i2r.a-star.edu.sg; ckgoh@i2r.a-star.edu.sg).
Z. N. Chen is with Department of Electrical and Computer Engineering, National University of Singapore, Singapore (e-mail: eleczn@nus.edu.sg).

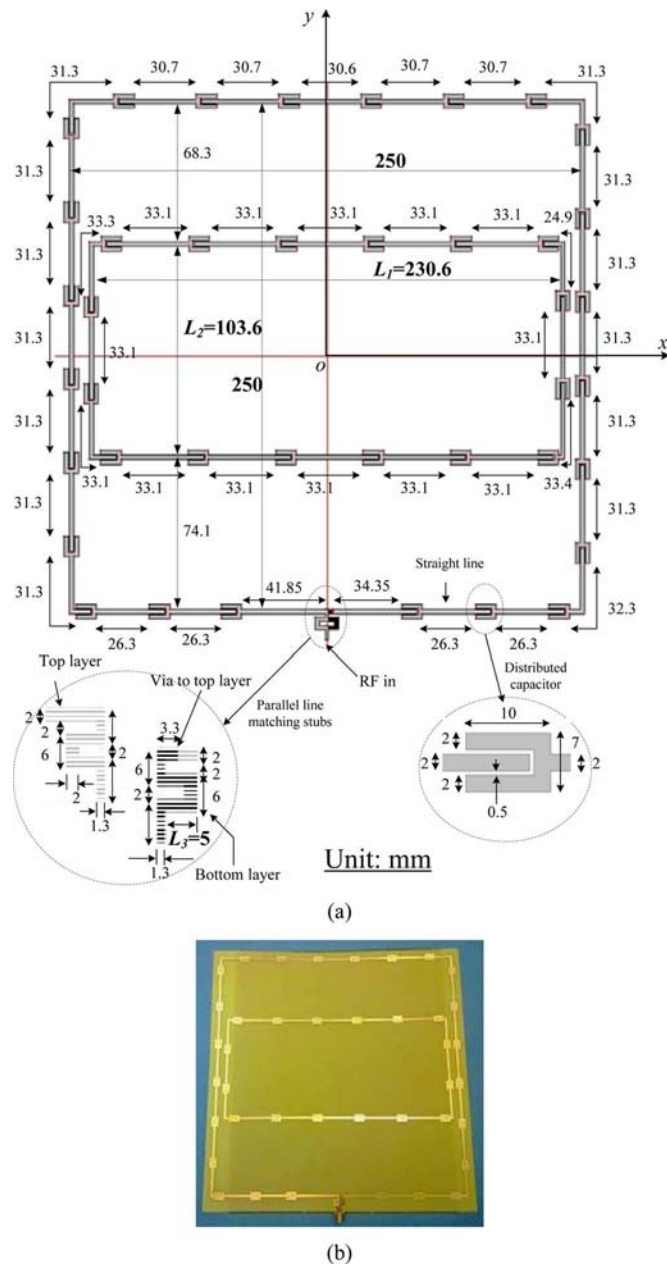Fig. 1.   Configuration of the dual-loop antenna. (a) Antenna with detailed dimension. (b) Photo of the antenna prototype using FR4 substrate.

Fig. 2.   Magnetic field distribution of the antenna with varying L_1 at 915 MHz along the (a) x-axis and (b) y-axis.

upper/bottom parallel strips are connected to the inner/outer conductors of a SubMiniature version A (SMA) connector, respectively.

The proposed antenna comprises a primary loop and a parasitic loop. The parasitic loop is positioned in the center of the primary loop to enhance the magnetic field strength there in order to generate the strong and uniform magnetic field distribution over a larger interrogation zone. Both loops comprise a number of segmented line sections which are able to provide a near-zero phase shift between the adjacent line sections. Each segmented line section is composed of a straight line and a distributed capacitor as shown in Fig. 1. For each loop with the required perimeter at the operating frequency, the geometrical
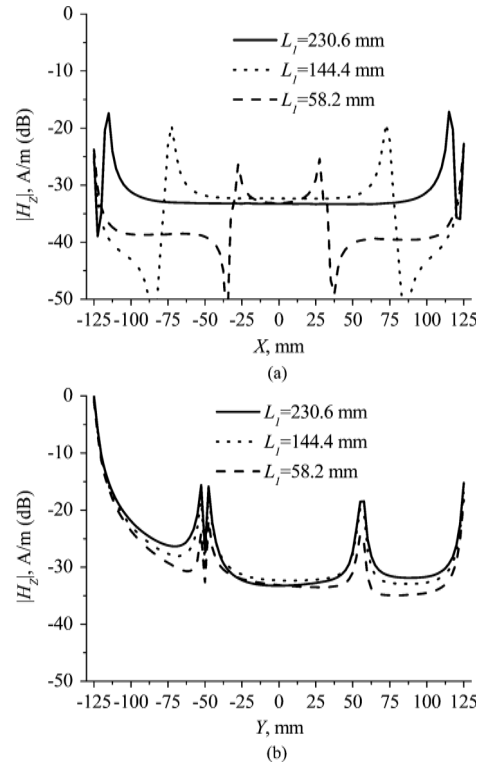
parameters of the loop can be determined in a way similar to those presented in [15] and [19].

B. Parameter Study

The parametric study is carried out to investigate the effect of the length (L_1) and width (L_2) of the parasitic loop on the magnetic field distribution of the dual-loop antenna as well as the effect of the length of the coplanar matching stub,L_3 on impedance matching of the proposed antenna. In the study, only one parameter is varied at a time while the others are kept unchanged unless it is indicated. The sides of the parasitic loop will symmetrically move outward or inward when L_1 and L_2 are increased or decreased, respectively, and the side length of the outer loop will remain unchanged. The antenna with the optimized geometrical parameters as shown in Fig. 1 is used as a reference. The parametric study was carried out by simulation using IE3D software [22].

Figs. 2 and 3 exhibit the magnetic field distributions ($|H_z|$) of the proposed dual-loop antenna with different L_1 and L_2 at 915 MHz, respectively. It is observed that L_1 affects the magnetic field distribution significantly, especially along the x-axis. A longer L_1 offers stronger and more uniform magnetic field distribution. Therefore, the left and right sides of the parasitic loop should be arranged close to the sides of the main loop. The width of the parasitic loop shows a slight effect on the magnetic field distribution along the x-axis. And L_2 should be optimized to enhance the magnetic field distribution along the y-axis. The peaks of the magnetic field strength near the segmented lines
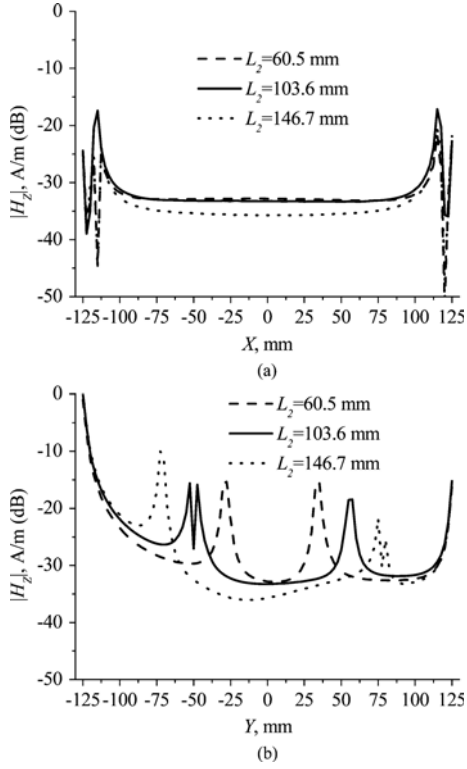
Fig. 3. Magnetic field distribution of the antenna with varying L_2 at 915 MHz along the (a) x-axis and (b) y-axis.
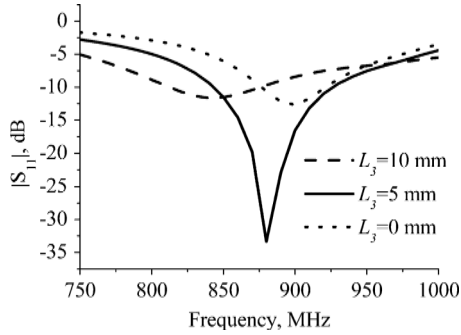

Fig. 4. Reflection coefficient of the proposed antenna with varying L_3.
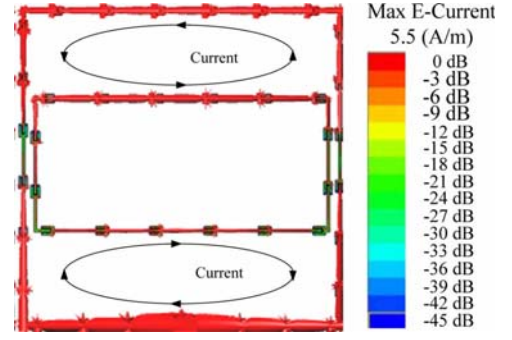

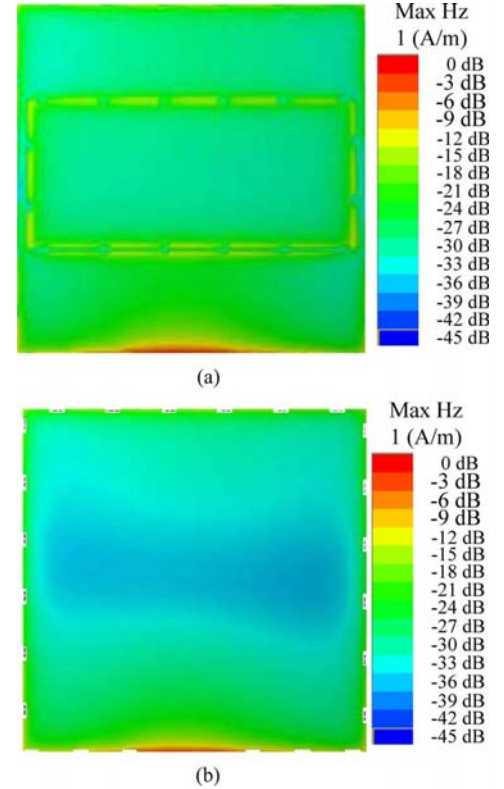Fig. 5. Simulated current distribution of the dual-loop antenna at 915 MHz.

Fig. 6. Simulated 2-D magnetic field distribution at 915 MHz ($z = 0.5$ mm): (a) the proposed dual-loop antenna and (b) single segmented loop.

of the parasitic loop result from the induced current on the segmented line sections of the parasitic loop from the main loop, so that the positions of the peaks will move when the size of the parasitic loop changes.

Fig. 4 shows the simulated $|S_{11}|$ of the proposed dual-loop antenna for different values of L_3. It can be seen that L_3 affects the impedance matching of the dual-loop antenna greatly. The desired impedance matching of the antenna can be achieved using the matching stubs as shown in Fig. 1.

C. Results

The antenna is optimized and prototyped with an overall size of 270 mm $\times$ 277 mm $\times$ 0.5 mm and offers an interrogation zone of 250 mm $\times$ 250 mm. The antenna prototype fabricated onto an FR4 PCB is shown in Fig. 1(b).

Current and Magnetic Field Distribution: Figs. 5 and 6(a) exhibit the simulated current distribution and the two-dimension (2-D) magnetic field distributions of the proposed dual-loop antenna at 915 MHz, respectively. From Fig. 5, it can be seen that the currents along each loop are no longer in-phase due to the coupling between the main loop and the parasitic loop. The area enclosed by the main loop is divided into three regions by the parasitic loop. The upper and lower portions of the antenna can be considered as the two loops with in-phase current. Therefore, a uniform magnetic field distribution can be achieved over these areas. In the central portion which is enclosed by the parasitic loop, the magnetic field is the superposition of the magnetic field generated by the primary loop as well as the parasitic loop. As a result, the strength of the magnetic field in the central portion of the antenna is comparable to that in the upper and lower portion. Therefore, the antenna can have strong magnetic field strength
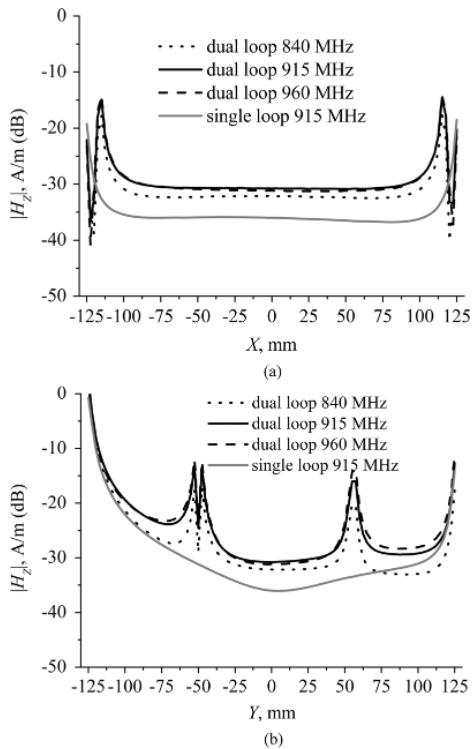
Fig. 7. Simulated magnetic field distribution of the dual-loop antenna proto-type at different frequencies ($z = 0.5$ mm): (a) x-axis variation and (b) y-axis variation.

Fig. 8. Simulated and measured magnetic field distributions of dual-loop antenna (915 MHz, $z = 0.5$ mm): (a) x-axis variation and (b) y-axis variation.

Fig. 9. Simulated and measured $|S_{11}|$ of the proposed dual-loop antenna.

in the whole antenna region even though the perimeter of the interrogation zone is three operating wavelengths as shown in Fig. 6(a).

For comparison, Fig. 6(b) shows the 2-D magnetic field distribution of a single segmented loop antenna wherein the antenna is identical to the main loop of the proposed antenna. The magnetic field at the central portion is greatly degraded compared with dual-loop antenna, although the current along the loop is in-phase.

Fig. 7 illustrates the simulated magnetic field distribution of the dual-loop antenna at 840, 915, and 960 MHz and the single segmented loop antenna at 915 MHz along the x- and y-axes, respectively. It is found that the proposed antenna achieves the uniform magnetic field distribution with a maximum variation of 3 dB at the interval of -95 mm $\leq x \leq 97.5$ mm and -32.5 mm $\leq y \leq 45$ mm and 62.5 mm $\leq y \leq 117.5$ mm across the frequency range of 840–960 MHz. It is obvious that the magnetic field of the single segmented loop antenna is much weaker than that of the proposed antenna along both the x- and y- axes, and the difference reaches 5 dB.

Fig. 8 compares the simulated and measured magnetic field distributions at 915 MHz. The magnetic field distribution was measured using an E5230A vector network analyzer (VNA), a power amplifier with the output power of 20 dBm, an HP8593E spectrum analyzer, and a near-field probe (Langer EMV-Technik RF-R 3–2) [23]. The continuous wave at 915 MHz is generated from the VNA to feed the antenna through the power amplifier, and the near-field probe is connected to the spectrum analyzer for quantifying the magnetic field intensity. The nea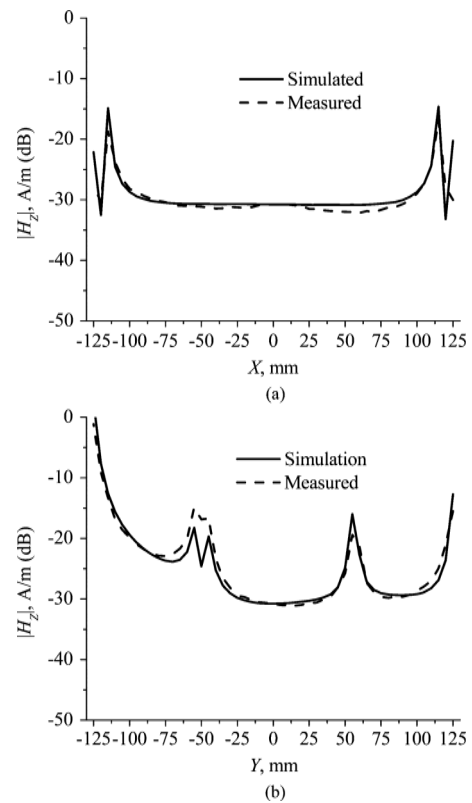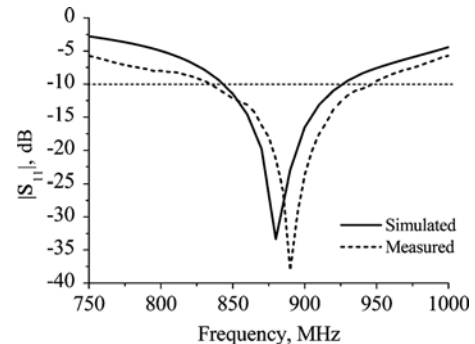r-field magnetic field probe was placed on the surface of the antenna prototype and moved along the x- and y- axes with an interval of 5 mm. The measured and simulated z-components of magnetic field are in good agreement. For brevity, the results at other frequencies are not exhibited here.

Impedance Matching: Fig. 9 shows the simulated and measured $|S_{11}|$ of the proposed dual-loop antenna. The -10-dB $|S_{11}|$ is from 845 to 928 MHz, or 9.36%. The measured result agrees well with the simulation. The slight shift of $|S_{11}|$ is believed to be caused by the fabrication error of the gaps of the distributed capacitors and the thickness of the substrate.

Reading Range: To verify the performance of the proposed antenna, the antenna prototype was used as the reader antenna in the UHF near field RFID system to detect UHF near-field tags. The system includes an Impinj Speedway reader operating at 902–928 MHz with 30-dBm output [24] and 80 button type tags (J12, 15×8 mm^2) [25]. In the measurement, the 80 tags were
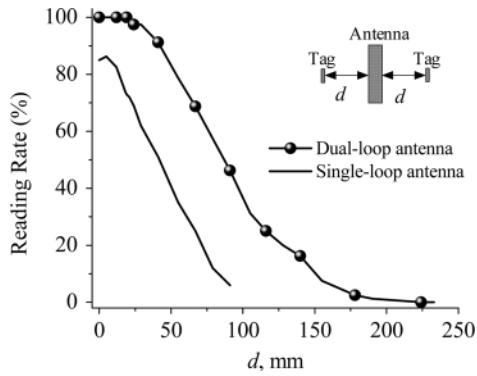
Fig. 10. Measured reading rate against reading range of the distributed capacitor loaded dual-loop antenna.

Fig. 11. Configuration of a square loop antenna with consistent current.

positioned symmetrically on a square sheet of Styrofoam with a side length of 250 mm. The number of the correctly detected tags was recorded when the Styrofoam square was positioned right above the antenna. To ensure the reliability of the results, the tags attached on the square Styrofoam were randomly placed on the antenna, and an average of five tests was recorded.

The measured reading rate against the reading range is exhibited in Fig. 10. The proposed antenna offers the bidirectional detection along the $\pm z$ axis. A 100% reading rate is achieved within a distance of 19 mm, while the reading rate of the single segmented loop antenna is greatly reduced at the same distance.

III. UPPER BOUND OF INTERROGATION ZONE OF A SINGLE SEGMENTED LOOP ANTENNA

The segmented antennas [11]–[21] are able to produce strong and uniform magnetic field distribution when the perimeter of the loop antenna is up to two wavelengths. However, a single segmented loop antenna is not able to further enlarge the interrogation zone because of the rapid attenuation of the field in the near-field region. There is an upper bound on the size of the segmented loop for a specific uniform magnetic field distribution even though the current along the loop is in-phase. As shown in Fig. 11, assume a square loop antenna with an ideal current distribution of consistent phase and amplitude along the loop. The loop is with a side length of a and the origin of the coordinate system is at the center of the square loop. The z-component of the magnetic field of a short current can be expressed as [26]

$$H_Z = \frac{I_0 L \sin\theta e^{-j\omega r/c}}{4\pi}\left(\frac{j\omega}{cr} + \frac{1}{r^2}\right) \quad (1)$$

where,

I_0 is the current,

L is the length of a short current,

r is the distance from the short current $(r \gg L)$,

θ is the elevation angle in the spherical coordinate,

ω is the angular frequency,
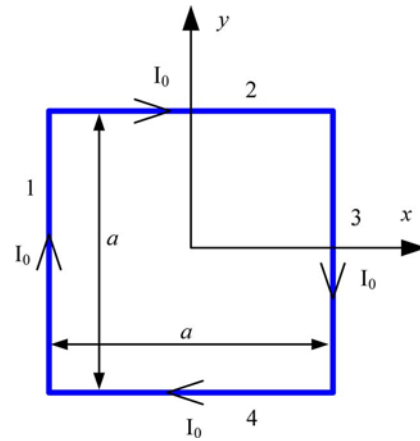
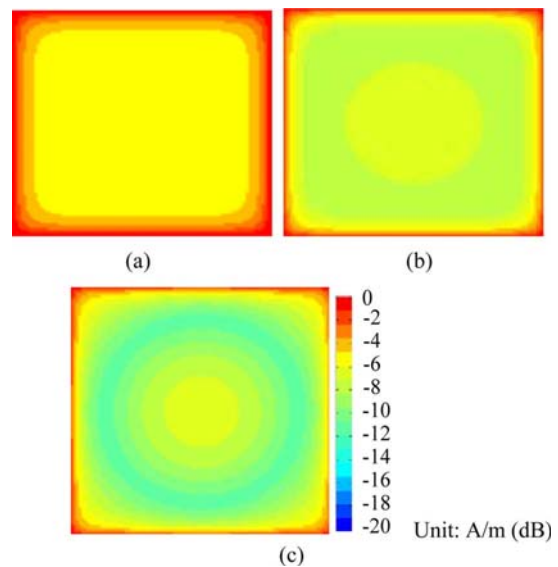c is the velocity of light in vacuum.

Fig. 12. Simulated 2-D magnetic field distribution of the square loop antenna with consistent current against perimeter of the loop. (a) two wavelengths; (b) three wavelengths; (c) four wavelengths.

The z-components (H_{Zi}, where i is the side number, and $i = 1, 2, 3$, or 4) of the magnetic field at any point (x, y) generated by each side of the loop antenna can be obtained by integrating the fields from all the short currents along the side. The magnetic field at any point inside the loop is the superposition of the fields from the four sides and can be concluded as

$$H_{Z\,\text{total}} = H_{Z1} + H_{Z2} + H_{Z3} + H_{Z4}. \quad (2)$$

Fig. 12 shows the calculated 2-D magnetic field distribution inside the loop area at z = 0 with different perimeters of $2\lambda, 3\lambda$ and 4λ. It can be seen that when the perimeter of the loop is larger, the magnetic field distribution inside the loop becomes weaker and features larger variation.

Fig. 13 shows the magnetic field distributions of the loop along the x-axis with the perimeters of $2\lambda, 3\lambda$ and 4λ. The maximum variations of the magnetic field distribution in the major portion of the antenna within the interval of $-0.36a \leq x \leq 0.36a$ are 0.5, 1.6, and 4.7 dB, respectively. Using the ratio of the 3-dB interval to the side length to evaluate the performance
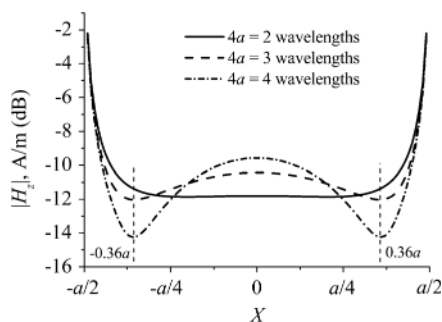
Fig. 13. Simulated magnetic field distributions along the x-axis of the ideal loop with different perimeters, where the values of x-axis is a relative value comparing to respective side length.

of the magnetic field distribution of a near-field antenna, the longer the perimeter is, the worse the near-field magnetic field distribution of the loop antenna is. This ratio for the ideal loop with a perimeter of 4λ only reaches to 44%. This ratio will be worse for a practical near-field loop antenna. It predicates that to realize an interrogation zone with the perimeter of 3λ is almost impossible using a single loop antenna. Therefore, the proposed dual-loop antenna is an appropriate solution for a UHF near-field antenna when the perimeter of its interrogation zone is required to be 3λ and even larger.

IV. CONCLUSION

Designing electrically-large UHF near-field RFID reader antennas is a big challenge, especially when the perimeter of interrogation zone is three wavelengths or more. The single segmented loop antenna is only able to offer an interrogation zone with a perimeter of two wavelengths. The proposed dual-loop antenna has demonstrated the capability of producing a strong and uniform field distribution in the near-field region of the antenna even for the perimeter of the interrogation zone up to three operating wavelengths. The introduction of the parasitic loop in the central region has significantly enlarged the interrogation zone so that the proposed antenna is promising for UHF near-field RFID reader applications.

REFERENCES

[1] R. Wantc, "An introduction to RFID technology," *IEEE Pervasive Comput.*, vol. 5, no. 1, pp. 25–33, Jan.–Mar. 2006.

[2] J. Landt, "The history of RFID," *IEEE Potentials*, vol. 24, no. 4, pp. 8–11, Oct.–Nov. 2005.

[3] K. Finkenzeller, *RFID Handbook*, 2nd ed. New York, NY, USA: Wiley, 2004.

[4] P. Harrop, New Field UHF vs. HF for Item Level Tagging [Online]. Available: http://www.eurotag.org/?Articles_and_Publications

[5] D. Desmons, "UHF Gen2 for Item-Level Tagging," presented at the RFID World, 2006 [Online]. Available: www.impinj.com/files/Impinj_ILT_RFID_World.pdf

[6] *UHF Gen 2 for Item-Level Tagging Impinj RFID Technology Series Paper* [Online]. Available: http://www.impinj.com/files/MR_GP_ED_0003_ILT.pdf

[7] C. Ajluni, "Item-level RFID takes off," *RF Design Mag.*, Sep. 2006.

[8] "Philips, TAGSYS, and Texas Instruments," [Online]. Available: http://www.tagsysrfid.com/moduals/tagsys/upload/news/TAGSYSTI-Philips_White-Paper.pdf

[9] P. V. Nikitin, K. V. S. Rao, and S. Lazar, "An overview of near field UHF RFID," in *Proc. IEEE Int. Conf. RFID*, Mar. 2007, pp. 167–174.

[10] S. Chen and V. Thomas, "Optimization of inductive RFID technology," in *Proc. IEEE Int. Symp. Electron. Environ.*, May 2001, pp. 82–87.

[11] D. M. Dobkin, S. M. Weigand, and N. Iyec, "Segmented magnetic antennas for near-field UHF RFID," *Microw. J.*, vol. 50, no. 6, Jun. 2007.

[12] R. A. Oliver, "Broken-Loop RFID Reader Antenna for Near Field and Far Field UHF RFID Tags," U.S. Design Patent D570, 337 S, Jun. 3, 2008.

[13] R. A. Oliver, "Broken-Loop RFID Reader Antenna for Near Field and Far Field UHF RFID Tags," U.S. Design Patent D574 369 S, Aug. 5, 2008.

[14] R. A. Oliver, "Broken-Loop RFID Reader Antenna for Near Field and Far Field UHF RFID Tags," U.S. Design Patent D574, 370 S, Aug. 5, 2008.

[15] Y. S. Ong, X. Qing, C. K. Goh, and Z. N. Chen, "A segmented loop antenna for UHF near-field RFID," in *Proc. IEEE Antennas Propag. Soc. Int. Symp.*, 2010, pp. 1–4.

[16] X. Qing, Z. N. Chen, and C. K. Goh, "UHF near-field RFID reader antenna with capacitive couplers," *IET Electron. Lett.*, vol. 46, no. 24, pp. 1591–1592, Dec. 2010.

[17] X. Qing, C. K. Goh, and Z. N. Chen, "Segmented loop antenna for UHF near-field RFID applications," *IET Electron. Lett.*, vol. 45, no. 17, pp. 872–873, Aug. 2009.

[18] X. Li, J. Liao, Y. Yuan, and D. Yu, "Segmented coupling eye-shape UHF band near field antenna design," in *Proc. IEEE Microw. Asia Pacific Conf.*, Singapore, Dec. 2009, pp. 2401–2404.

[19] X. Qing, C. K. Goh, and Z. N. Chen, "A broadband near-field UHF RFID antenna," *IEEE Trans. Antennas Propag.*, vol. 58, no. 12, pp. 3829–3838, Dec. 2010.

[20] Z. N. Chen, C. K. Goh, and X. Qing, "Loop antenna for UHF near-field RFID reader," in *Proc. 4th Eur. Conf. Antenna Propag.*, Barcelona, Spain, Apr. 2010, pp. 1–4.

[21] X. Li and Z. Yang, "Dual-printed-dipoles reader antenna for UHF near-field RFID applications," *IEEE Antenna Wireless Propag. Lett.*, vol. 10, pp. 239–242, 2011.

[22] Zeland Software Inc., "IE3D user's manual release 12," . Fremont, CA, USA, Oct. 2006.

[23] [Online]. Available: http://www.langer-emv.de/en/products/disturbance-emission/mear-fieldprober/rf-1/

[24] [Online]. Available: http://www.impini.com/products/rfid-reader.aspx

[25] Tag Antenna Designs [Online]. Available: http://www.rfid-info.jp/whitepaper/379.pdf

[26] J. D. Kraus and R. J. Marhefka, *Antennas for All Applications*, 3rd ed. New York, NY, USA: McGraw-Hill Science, 2001.

Jin Shi received the B.Sc. degree from HuaiYin Teachers College, Huai'an City, China, in 2001, the M.Sc. degree from the University of Electronic Science and Technology of China (UESTC), Chengdu, China, in 2004, and the Ph.D. degree from City University of Hong Kong, Hong Kong, in 2011.

During 2004–2006, he was a Research Engineer working on RF repeater system. During 2007–2008, he was a Research Assistant of the City University of Hong Kong. Since 2011, he has worked at the Institute for Infocomm Research, Singapore, where his current appointments are Scientist. His current research interests are RF/microwave components and subsystems, near-field antennas, millimeter-wave filters and antennas, and radio frequency identification (RFID) systems.

Xianming Qing (M'88) received the B.Eng. degree from the University of Electronic Science and Technology of China (UESTC), Chengdu, China, in 1985, and the Ph.D. degree from Chiba University, Chiba, Japan, in 2010.

During 1987–1996, he was with UESTC for teaching and research and appointed as a Lecturer in 1990, and an Associate Professor in 1995. He joined National University of Singapore (NUS) in 1997 as a Research Scientist. Since 1998, he has been with the Institute for Infocomm Research (I^2R, formerly known as CWC and ICR), Singapore. He is currently holding the position of Senior Scientist and Leader of the Antenna Group under the RF and Optical Department. His main research interests are antenna design and characterization for wireless applications. In particular, his current R&D focuses on small and broadband antennas/arrays for wireless systems, such as ultra-wideband (UWB) systems, radio frequency identification (RFID) systems

and medical imaging systems, microwave, mmW, submmW, and THz imaging systems. He has authored and coauthored over 130 technical papers published in international journals or presented at international conferences, and five book chapters. He holds 10 granted and filed patents.

Dr. Qing has been a Member of the IEEE Antennas and Propagation Society since 1990. He received six awards of advancement of science and technology in China. He is also the recipient of the IES 2006 Prestigious Engineering Achievement Award, Singapore, and the ISAP 2010 Best Paper Award. He has served as a member for the RFID Technical Committee (TC-24) of the IEEE MTT since 2009 and served as the Organizer and Chair for special sessions on RFID antennas at the IEEE Antenna and Propagation Symposium in 2007 and 2008. He is serving as an Editorial Board Member for the *International Journal of Microwave Science and Technology*. He also served as the Guest Editor of the Special Issue "Antennas for Emerging Radio Frequency Identification (RFID) Applications" of the *International Journal on Wireless & Optical Communications*. He has served as a TPC member and Session Chair for a number of conferences, and as a reviewer for many prestigious journals such as the IEEE TRANSACTIONS ON ANTENNAS AND PROPAGATION, the IEEE TRANSACTIONS ON MICROWAVE THEORY AND TECHNOLOGY, the IEEE ANTENNAS AND WIRELESS PROPAGATION LETTERS, *MWCL, IET-MAP, Electronic Letters*, etc.

Zhi Ning Chen (F'05) received the B.Eng., M.Eng., and Ph.D. degrees from the Institute of Communications Engineering (ICE), China, all in electrical engineering, and the Ph.D. degree from University of Tsukuba, Tsukuba, Japan, respectively.

During 1988–1995, he worked at ICE as a Lecturer and later as an Associate Professor, also during this time he was with Southeast University, China, as a Postdoctoral Fellow and later as an Associate Professor. During 1995–1997, he joined the City University of Hong Kong as a Research Assistant and later as a Research Fellow. In 1997, he was awarded the Japan Society for the Promotion of Science (JSPS) Fellowship to conduct his research at the University of Tsukuba, Japan. In 2001 and 2004, he visited the University of Tsukuba under a JSPS Fellowship Program (senior level). In 2004, he worked at IBM T. J. Watson Research Center, as an Academic Visitor. During 1999–2012, he worked with the Institute for Infocomm Research (I^2R) (formerly known as Centre for Wireless Communications and Institute for Communications Research) as a Member of Technical Staff (MTS), Senior MTS, Principal MTS, Senior Scientist, Lead Scientist, and Principal Scientist as well as Head of the RF & Optical Department. In June 2012, he joined the Department of Electrical and Computer Engineering, National University of Singapore, as a Full Professor and is concurrently holding a joint appointment as Advisor at I^2R as well as Visiting/Adjunct/Guest Professor positions at Southeast University, Nanjing University, Shanghai Jiaotong University, Tsinghua University, Tongji University, University of Science and Technology of China, Dalian Maritime University, Chiba University, National Taiwan University of Science and Technology as well as City University of Hong Kong. His current research interest includes electromagnetic engineering as well as the antennas for communication, radar, imaging, and sensing systems. He has published more than 400 technical papers and authored/edited four books entitled *Broadband Planar Antennas*, *UWB Wireless Communication*, *Antennas for Portable Devices*, and *Antennas for Base Stations in Wireless Communications*. He also contributed chapters to the books entitled *UWB Antennas and Propagation for Communications, Radar, and Imaging*, *Antenna Engineering Handbook* as well as *Microstrip and Printed Antennas*. He currently holds 29 granted and filed patents with 33 licensed deals with industry.

Dr. Chen is the recipient of International Symposium on Antennas and Propagation Best Paper Award 2010, the CST University Publication Award 2008, IEEE AP-S Honorable Mention Student Paper Contest 2008, IES Prestigious Engineering Achievement Award 2006, I^2R Quarterly Best Paper Award 2004, and IEEE iWAT 2005 Best Poster Award. He is an Associate Editor for the IEEE TRANSACTIONS ON ANTENNAS AND PROPAGATION and was a Distinguished Lecturer for the IEEE Antennas and Propagation Society during 2009–2011. He was the founding General Chair of the International Workshop on Antenna Technology (iWAT), International Symposium on InfoComm & Media Technology in Bio-Medical & Healthcare Applications (IS 3T-in-3A), International Microwave Forum (IMWF), as well as Asia-Pacific Conference on Antennas and Propagation (APCAP).

Chean Khan Goh received the M.Eng. degree from the National University of Singapore, Singapore, in 2009. He is currently working toward the Ph.D. degree at the National University of Singapore.

He works as a Research Engineer in Institute for Infocomm Research, Singapore, since 2007. His research interests include near-field antennas for RFID application, antennas for body-centric communications, and antenna impedance measurement methodology.